

# Three-dimensional inverse energy cascade induced by vortex reconnections

A. W. Baggaley,<sup>1,2</sup> C. F. Barenghi,<sup>3</sup> and Y. A. Sergeev<sup>4</sup>

<sup>1</sup>*School of Mathematics and Statistics, University of Glasgow, Glasgow, G12 8QW, UK*

<sup>2</sup>*Joint Quantum Centre Durham-Newcastle, School of Mathematics and Statistics,  
Newcastle University, Newcastle upon Tyne, NE1 7RU, UK*

<sup>3</sup>*Joint Quantum Centre Durham-Newcastle, School of Mathematics and Statistics,  
University of Newcastle, Newcastle upon Tyne, NE1 7RU, UK*

<sup>4</sup>*Joint Quantum Centre Durham-Newcastle, School of Mechanical and Systems Engineering,  
Newcastle University, Newcastle upon Tyne, NE1 7RU, UK*

A recent study of homogeneous isotropic turbulence by Biferale, Musacchio and Toschi has determined that a three-dimensional inverse energy cascade is possible if the nonlinearity of the Navier-Stokes equation is restricted in Fourier space to helical modes of the same sign. In low-temperature superfluid helium, viscosity is zero, vorticity takes the form of discrete, thin vortex filaments of fixed circulation, and turbulence is a tangle of such filaments. We exploit the simpler nature of quantum vorticity to show that the three-dimensional inverse energy cascade can arise from reconnections of vortex loops of the same polarity which shift energy from small length scales to large length scales, in analogy to what was envisaged by Biferale and collaborators in classical Navier-Stokes turbulence. We discuss superfluid turbulence experiments and the observed generation of the classical Kolmogorov energy spectrum in view of this finding.

PACS numbers: 67.25.dk, 47.37.+q 47.27.-i

The phenomenology of three-dimensional turbulence is based on Richardson's idea [17] of the (forward) turbulent cascade: kinetic energy, injected externally, feeds large eddies, which interact, become stretched and deformed into smaller and smaller eddies, until, at sufficiently small length scales, viscous forces dissipate this energy into heat. A reversed flux of energy, from the small scales to the large scales, is observed in two-dimensional turbulence [12, 22]. Such inverse cascade is rare in three-dimensional turbulence, but can be observed in the presence of strong anisotropy [9, 10, 25, 26], or when rotation [13, 15, 21] or confinement in layers [24] make the flow almost two-dimensional.

Recently, Biferale *et al.* [6] numerically induced the three-dimensional inverse energy cascade by artificially restricting the nonlinearity of the governing Navier-Stokes equation to the interaction of Fourier modes of the same helical sign. Their result clarifies previous observations and shows that, in principle, all three-dimensional turbulent flows contain nonlinearities which may lead to an inverse cascade: to make the effect apparent one has to break the mirror symmetry of the interactions.

The aim of this report is to exploit the unusual properties of superfluid helium and consider the three-dimensional inverse energy cascade in a quantum fluid setting in view of the finding of Biferale *et al.* [6]. At temperatures below 1 K, liquid helium ( $^4\text{He}$ ) is a pure superfluid. Unlike ordinary fluids (in which vorticity is a continuous field), the superfluid's rotational motion is constrained by quantum mechanics to discrete vortex lines of fixed circulation and atomic thickness. Vortex lines reconnect if they come sufficiently close to each other [11, 14]. In a recent experiment, Walmsley & Golov [23] used high voltage tips to inject vortex rings into  $^4\text{He}$  at very low temperatures, creating turbulence and monitoring its decay. Depending on the duration of the injection time, they found two decay regimes, characterized by distinct power laws. In a related experiment, Bradley *et al.* [7] used a vibrating grid to inject vortex loops into the isotope  $^3\text{He-B}$  (a fermionic superfluid), and observed the same power laws seen by Walmsley & Golov. We shall demonstrate that, in conditions typical of superfluid turbulence experiments, reconnections of vortex loops with the same polarity induce a three-dimensional inverse energy cascade, thus providing Biferale's spectral argument with a simple, striking example in real physical space.

We model vortex lines as space curves  $\mathbf{s}(\xi, t)$ , where  $\xi$  is arc length and  $t$  is time, which move according to the Biot-Savart law [18]:

$$\frac{d\mathbf{s}}{dt} = -\frac{\kappa}{4\pi} \oint_{\mathcal{L}} \frac{(\mathbf{s} - \mathbf{r})}{|\mathbf{s} - \mathbf{r}|^3} \times d\mathbf{r}, \quad (1)$$

where  $\kappa = 9.97 \times 10^{-4} \text{ cm}^2/\text{s}$  is the quantum of circulation in  $^4\text{He}$ , and the line integral extends over the entire vortex configuration  $\mathcal{L}$ . Our calculations are performed in a periodic cube of size  $D = 1 \text{ cm}$ . The numerical techniques to discretize vortex lines into a variable number of points  $N$  held at minimum separation  $\delta/2 = 0.01 \text{ cm}$ , compute the time evolution, de-singularize the Biot-Savart integrals, evaluating them using a tree-method (with critical opening angle 0.4), and the algorithm for vortex reconnections, are all described in the literature [1–4, 19].

The initial condition at  $t = 0$  consists of vortex rings of random size taken from a distribution with mean radius  $\bar{R} = 0.1 \text{ cm}$  and standard deviation  $\sigma = 0.047 \text{ cm}$ ; the rings, randomly placed in the computational box, are initially parallel to the  $xy$ -plane and travel in the positive  $z$ -direction. No further energy is injected into the vortex configuration. During the time evolution, the total energy slowly decreases because of numerical dissipation: the finite discretization along the vortex lines, controlled by the parameter  $\delta$ , damps high frequency Kelvin waves, and the vortex reconnection algorithm, again controlled by  $\delta$ , removes vortex length. These numerical effects play a dissipative role similar to phonon emission in the real physical system (kinetic energy is turned into sound energy which is radiated away). In order to highlight the three-dimensional inverse energy cascade, the initial condition used here is simpler than the initial condition that we used to model [5] the experiment of Walmsley & Golov [23] as realistically as possible (vortex rings were injected continually for a given period of time in the form of a narrow beam).

We present the numerical results. Fig. 1 shows that, starting from the initial condition, the vortex rings interact, reconnect and quickly form a vortex tangle. The time evolution of the vortex line density  $L$  is shown in Fig. 2. We analyze the build-up of the energy spectrum  $E(k)$ , which is defined by

$$\frac{1}{V} \int \frac{1}{2} \mathbf{v}^2 dV = \int_0^\infty E(k) dk, \quad (2)$$

where  $\mathbf{v}$  is the velocity field generated by the vortex lines,  $k = |\mathbf{k}|$  is the magnitude of the three-dimensional wavenumber and  $V = D^3$  is volume. Fig. 3 shows that at  $t = 0$  the energy is concentrated at  $k \approx 2\pi/2\bar{R} \approx 30 \text{ cm}^{-1}$  corresponding to the initial vortex rings. Our main finding is that, during the evolution, the energy spectrum  $E(k)$

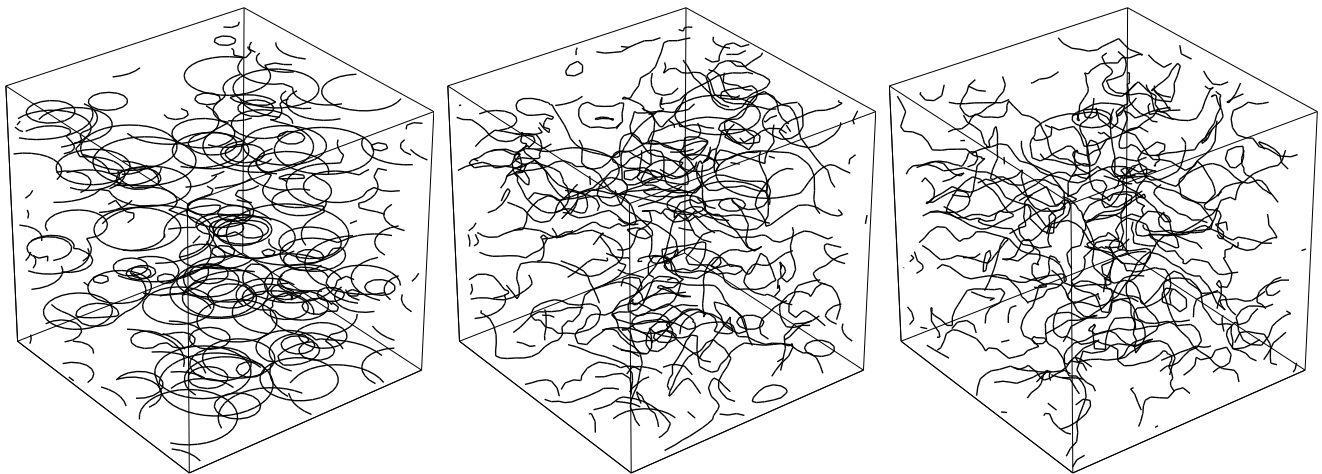


FIG. 1. Snapshots of the vortex tangle at  $t = 0$  (left),  $t = 10$  s (middle) and  $t = 20$  s (right)

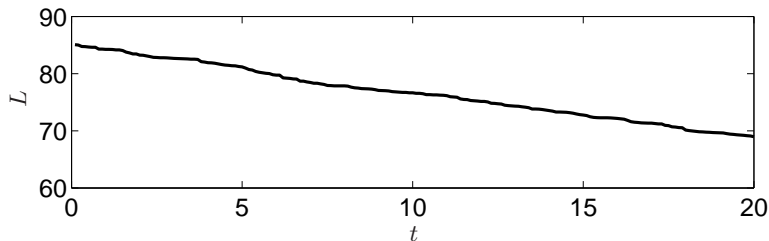


FIG. 2. Vortex line density  $L$  ( $\text{cm}^{-2}$ ) vs time  $t$  (s).

increases at small wavenumbers  $k < 30 \text{ cm}^{-1}$  and decreases at large wavenumbers  $k > 30 \text{ cm}^{-1}$ . This transfer of energy from small scales to large scales (inverse energy cascade) is also visible in Fig. 4 where we plot the energy flux  $\epsilon(k) = \int_{k_D}^k dE(k')/dt dk'$  where  $k_D = 2\pi/D$ .

We argue that this inverse energy cascade arises from reconnections of vortex lines. The interaction of two vortex lines occurs either indirectly via the velocity fields which they generate (the Biot-Savart law), or directly via vortex reconnections. To isolate the role played by vortex reconnections we repeat the calculation, replacing the Biot-Savart law with its Local Induction Approximation (LIA) [8, 16]:

$$\frac{ds}{dt} \approx \frac{\kappa}{4\pi} \ln(R/a_0) \mathbf{s}' \times \mathbf{s}'', \quad (3)$$

where a prime denotes derivative with respect to arc length,  $R = 1/|\mathbf{s}''|$  is the local radius of curvature and  $a_0 \approx 10^{-8} \text{ cm}$  is the vortex core radius in  $^4\text{He}$ . Under LIA, the vortex lines ignore each others' velocity fields and interact only when they reconnect. Fig. 5 shows that the inverse energy cascade is still present under LIA.

The following simple geometrical consideration captures the role of vortex reconnections on the scale-to-scale energy transfer. Energy and speed of a vortex loop of size  $R$  are roughly proportional to  $R$  and  $1/R$  respectively. A head-on collisions of two vortex loops forms two loops of approximately the same size (see Fig. 6 top). A collision from behind of two vortex loops travelling in the same direction (see Fig. 6 bottom) forms a larger vortex loop which contains most of the energy (and which, being slow, is likely to be hit by other loops, thus becoming entangled), and a smaller, less energetic loop (which moves away and is likely to be absorbed by the walls). Clearly, the first type of collisions tends to leave length scales unaltered, and the second type tends to shift energy to larger length scales.

When modelling the experiment of Walmsley & Golov [23] [5], we found that a short injection time was followed by a decay of the form  $L \sim t^{-1}$ , and a long injection time was followed by a decay of the form  $L \sim t^{-3/2}$ , as observed in the experiment. It has been argued that the first decay is typical of random superfluid turbulence, such that the

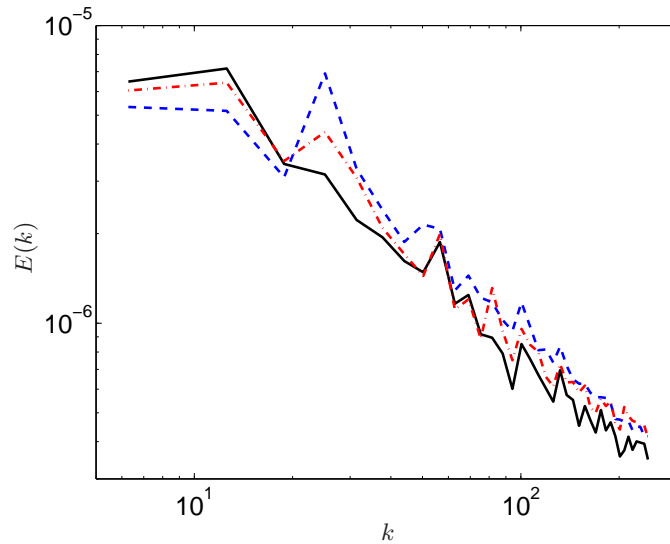


FIG. 3. (Color online) Energy spectrum  $E(k)$  (arbitrary units) vs wavenumber  $k$  ( $\text{cm}^{-1}$ ) at  $t = 0$  (dashed blue line),  $t = 10$  s (dot-dashed red line) and  $t = 20$  s (solid black line). Note the progressive increase of kinetic energy at small wavenumbers  $k < 30 \text{ cm}^{-1}$  and the decrease at large wavenumbers. The energy spectra are computed from a  $512^2$  Cartesian mesh in the  $xz$ -plane.

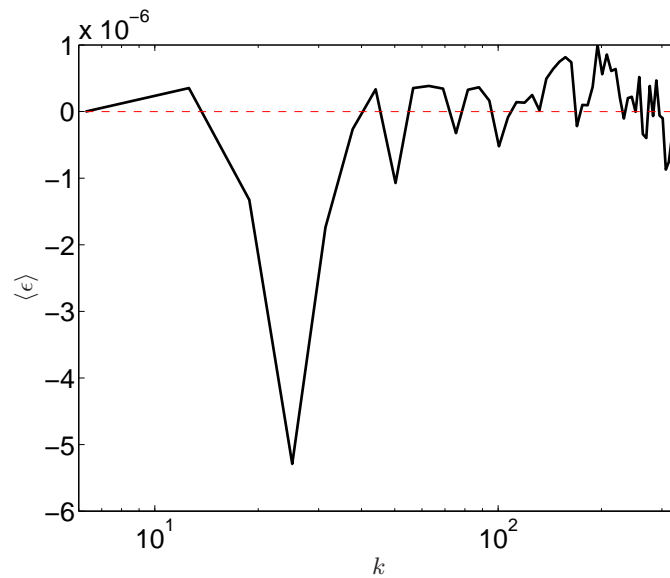


FIG. 4. Time averaged energy flux,  $\langle \epsilon \rangle$  (arbitrary units) vs wavenumber ( $\text{cm}^{-1}$ ).

only length scale present is the average intervortex distance  $\ell \approx L^{-1/2}$ , and the second decay of more structured, quasi-classical turbulence [20].

We now examine what happens if vortex loops are injected continually (by a vibrating grid for example), rather than given as initial condition and allowed to decay. Starting from an empty computational domain, we inject vortex rings with size drawn from the same normal distribution used earlier ( $\bar{R} = 0.1 \text{ cm}$ ,  $\sigma = 0.047 \text{ cm}$ ) with a frequency of 125Hz. The rings are injected in the  $yz$ -plane and travel in the positive  $x$  direction; their evolution is computed with the full Biot-Savart law. Figure 7 shows snapshots of the vortex tangle as the simulation progresses. We track the evolution of the energy spectrum, and find that the inverse cascade is very capable of transferring sufficient energy to low  $k$  that a spectrum consistent with the Kolmogorov  $k^{-5/3}$  scaling is built up, see Fig. 8. We remark that,

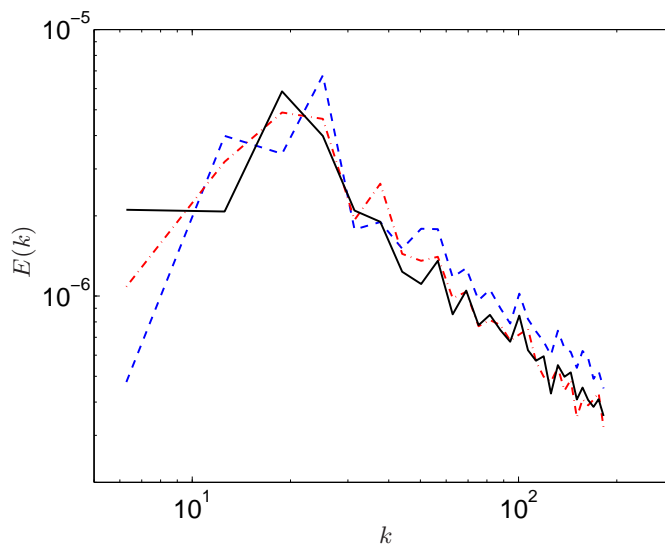


FIG. 5. (Color online) Energy spectrum  $E(k)$  (arbitrary units) vs wavenumber  $k$  ( $\text{cm}^{-1}$ ) at  $t = 0$  (dashed blue line),  $t = 10$  s (dot-dashed red line) and  $t = 20$  s (solid black line) for the calculation performed with LIA. Note again the progressive increase of energy at small wavenumbers.

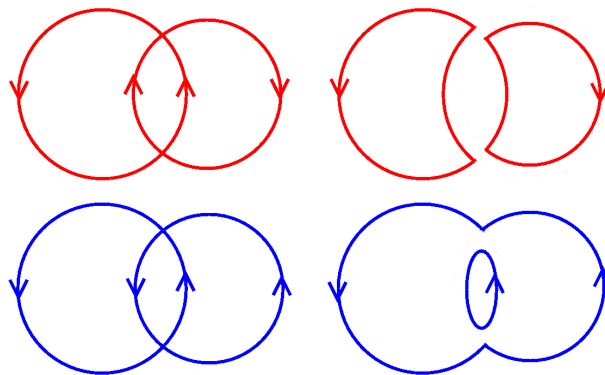


FIG. 6. Schematic head-on collision of vortex rings travelling in opposite direction (red, top) and collision from behind of vortex rings travelling in the same direction (blue, bottom), and resulting vortex configuration after the vortex reconnection.

in contrast to our early work [5] which modelled the conditions of the experiment of Walmsley & Golov [23], the injection is not in the form of a narrow beam from a single point (which may induce a large scale motion by itself), but is uniform in the  $yz$ -plane: the build-up of energy at small  $k$  is thus due only to the inverse cascade. Once the Kolmogorov spectrum is formed, if the injection of rings is stopped, the vortex line density decays as  $L \sim t^{-3/2}$ , as observed in the experiments [7, 23] and in numerical calculations [5].

In conclusion, superfluid turbulence experiments such as those of Walmsley & Golov [23] and of Bradley *et al.* [7] involve injecting a beam of vortex loops into the experimental cell, creating an initial anisotropy. This set-up creates a condition which favours the interaction and reconnection of vortex loops of the same polarity (which tends to transfer energy to larger length scales) and suppresses the head-on interaction of loops of the opposite polarity (which tends to leave the length scales unchanged). In physical space, this selection mechanism is analogue to the decimation procedure applied by Biferale *et al.* [6] in Fourier space to the Navier-Stokes equation, which suppressed the interaction of helical modes with different sign, and induces the inverse energy cascade.

We acknowledge fruitful discussions with W.F. Vinen, J. Laurie and S. Nazarenko, and the financial support of the Leverhulme Trust and the EPSRC.

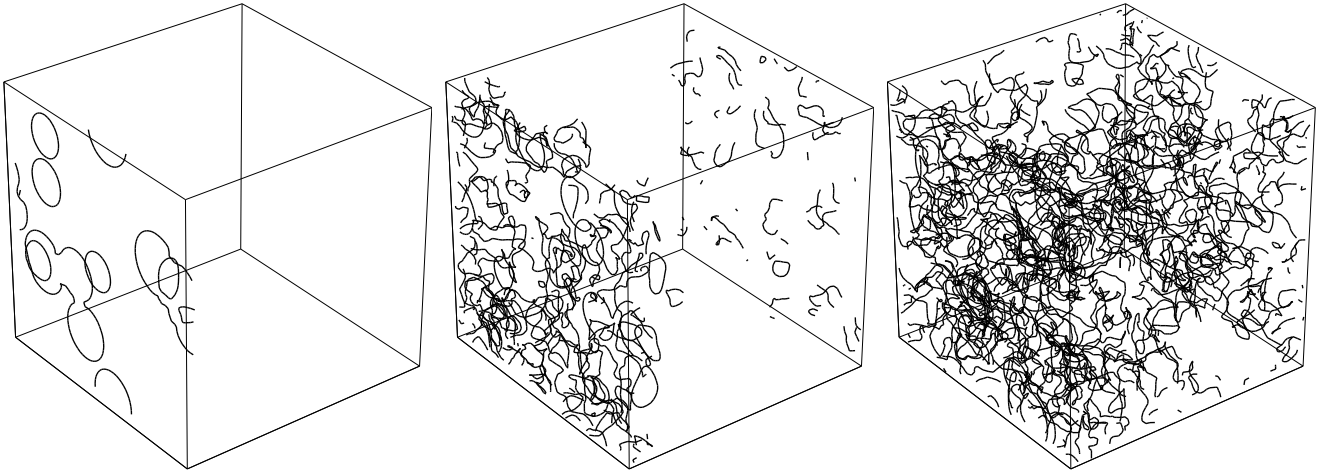


FIG. 7. Snapshots of the vortex tangle, due to loop injection at  $t = 0.075$  s (left),  $t = 0.1$  s (middle) and  $t = 15$  s (right)

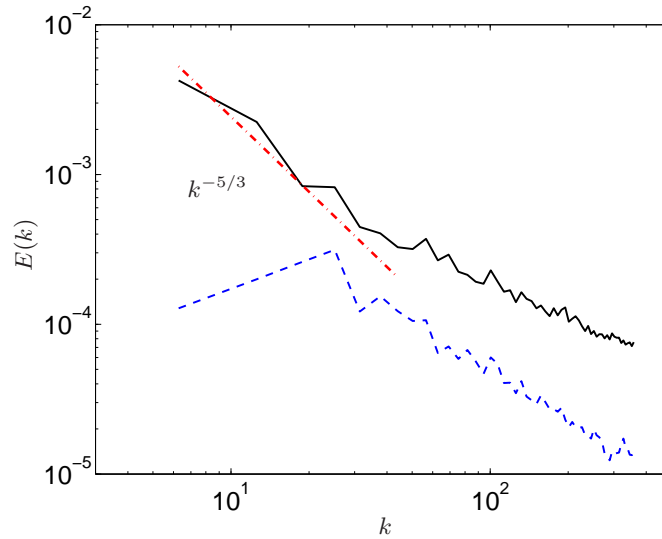


FIG. 8. (Color online) Energy spectrum  $E(k)$  (arbitrary units) vs wavenumber  $k$  ( $\text{cm}^{-1}$ ) at  $t = 0.75$  s,  $L = 43.9 \text{ cm}^{-2}$ , (dashed blue line) and  $t = 15$  s,  $L = 159.6 \text{ cm}^{-2}$ , (solid black line) corresponding to a continual injection of vortex rings, see Fig. 7. Note the formation of the Kolmogorov  $k^{-5/3}$  spectrum, indicated by the dot-dashed red line.

- 
- [1] BAGGALEY, A. 2012 The sensitivity of the vortex filament method to different reconnection models. *Journal of Low Temperature Physics* **168**, 18–30.
  - [2] BAGGALEY, A. & BARENGHI, C. 2012 Tree method for quantum vortex dynamics. *Journal of Low Temperature Physics* **166**, 3–20.
  - [3] BAGGALEY, ANDREW W. & BARENGHI, CARLO F. 2011 Spectrum of turbulent kelvin-waves cascade in superfluid helium. *Phys. Rev. B* **83**, 134509.
  - [4] BAGGALEY, A. W. & BARENGHI, C. F. 2011 Vortex-density fluctuations in quantum turbulence. *Phys. Rev. B* **84**, 020504.
  - [5] BAGGALEY, A. W., BARENGHI, C. F. & SERGEEV, Y. A. 2012 Quasiclassical and ultraquantum decay of superfluid turbulence. *Phys. Rev. B* **85**, 060501.
  - [6] BIFERALE, LUCA, MUSACCHIO, STEFANO & TOSCHI, FEDERICO 2012 Inverse energy cascade in three-dimensional isotropic turbulence. *Phys. Rev. Lett.* **108**, 164501.
  - [7] BRADLEY, D. I., CLUBB, D. O., FISHER, S. N., GUÉNAULT, A. M., HALEY, R. P., MATTHEWS, C. J., PICKETT, G. R.,

- TSEPELIN, V. & ZAKI, K. 2006 Decay of pure quantum turbulence in superfluid  $^4\text{He}$  –  $b$ . *Phys. Rev. Lett.* **96**, 035301.
- [8] DA RIOS, LUIGI 1906 Sul moto dun liquido indefinito con un filetto vorticoso di forma qualunque. *Rendiconti del Circolo Matematico di Palermo (1884 - 1940)* **22**, 117–135.
- [9] GALANTI, B. & SULEM, P.-L. 1991 Inverse cascades in three-dimensional anisotropic flows lacking parity invariance. *Physics of Fluids A: Fluid Dynamics* **3** (7), 1778–1784.
- [10] HEFER, DAVID & YAKHOT, VICTOR 1989 Inverse energy cascade in a time-dependent flow. *Physics of Fluids A: Fluid Dynamics* **1** (8), 1383–1386.
- [11] KOPLIK, JOEL & LEVINE, HERBERT 1993 Vortex reconnection in superfluid helium. *Phys. Rev. Lett.* **71**, 1375–1378.
- [12] KRAICHNAN, R. H. & MONTGOMERY, D. 1980 Two-dimensional turbulence. *Reports on Progress in Physics* **43** (5), 547.
- [13] MININNI, P. D. & POUQUET, A. 2010 Rotating helical turbulence. i. global evolution and spectral behavior. *Physics of Fluids* **22** (3), 035105.
- [14] PAOLETTI, M.S., FISHER, MICHAEL E. & LATHROP, D.P. 2010 Reconnection dynamics for quantized vortices. *Physica D: Nonlinear Phenomena* **239** (14), 1367 – 1377, [jce:title¿At the boundaries of nonlinear physics, fluid mechanics and turbulence: where do we stand? Special issue in celebration of the 60th birthday of K.R. Sreenivasani¿ce:title¿](#).
- [15] POUQUET, A., SEN, A., ROSENBERG, D., MININNI, P. D. & BAERENZUNG, J. 2012 Inverse cascades in turbulence and the case of rotating flows. *ArXiv e-prints* .
- [16] RICCA, RENZO L. 1996 The contributions of Da Rios and Levi-Civita to asymptotic potential theory and vortex filament dynamics. *Fluid Dynamics Research* **18** (5), 245.
- [17] RICHARDSON, L. F. 1922 *Weather Prediction by Numerical Process*. Cambridge University Press.
- [18] SAFFMAN, P. G. 1992 *Vortex Dynamics*. Cambridge University Press.
- [19] SCHWARZ, K. W. 1988 Three-dimensional vortex dynamics in superfluid  $^4\text{He}$ : Homogeneous superfluid turbulence. *Phys. Rev. B* **38**, 2398–2417.
- [20] SKRBEK, L. & SREENIVASAN, K. R. 2012 Developed quantum turbulence and its decay. *Physics of Fluids* **24** (1), 011301.
- [21] SMITH, LESLIE M. & WALEFFE, FABIAN 1999 Transfer of energy to two-dimensional large scales in forced, rotating three-dimensional turbulence. *Physics of Fluids* **11** (6), 1608–1622.
- [22] TABELING, PATRICK 2002 Two-dimensional turbulence: a physicist approach. *Physics Reports* **362** (1), 1 – 62.
- [23] WALMSLEY, P. M. & GOLOV, A. I. 2008 Quantum and quasiclassical types of superfluid turbulence. *Phys. Rev. Lett.* **100**, 245301.
- [24] XIA, H., PUNZMANN, H., FALKOVICH, G. & SHATS, M. G. 2008 Turbulence-condensate interaction in two dimensions. *Phys. Rev. Lett.* **101**, 194504.
- [25] YAKHOT, VICTOR & PELZ, RICHARD 1987 Large-scale structure generation by anisotropic small-scale flows. *Physics of Fluids* **30** (5), 1272–1277.
- [26] YAKHOT, V. & SIVASHINSKY, G. 1987 Negative-viscosity phenomena in three-dimensional flows. *Phys. Rev. A* **35**, 815–820.